Skid Steering in 4WD EV

Gao Shuang, Norbert C. Cheung, Eric K. W. Cheng, Dong Lei, Liao Xiaozhong

Abstract--This paper discusses skid steering applied to four wheel drive electric vehicles. In such vehicles, steering is achieved by differentially varying the speeds of the lines of wheels on different sides of the vehicle in order to induce yaw. Skid steer wheeled vehicles require elaborate tire model, so I choose the unite semi-empirical tire model. From this model, longitudinal and lateral tire force can be calculated by slip ratio directly. The vehicle model has 3-DOF, longitudinal, lateral and yaw direction, irrespective of suspension. Induction motor is chosen as the driven motor, and the control method is rotor flux field oriented vector control. To satisfy the requirement of the turn radius, the longitudinal slip must be controlled, so a method of slip limitation feedback is used in the simulation. When the vehicle is turning on a slippery surface, because of the drop at the coefficient of road adhesion, the drive wheels may slip. The traction control system reduces the engine torque and brings the slipping wheels into the desirable skid range. Some simulation results about the steering accuracy and maneuverability are given in the paper.

Index Terms--Skid steer, electric vehicle, induction motor, vector control

I. INTRODUCTION

AS is known to all, for skid steering vehicle, all of the wheels are non-steerable, and lateral slippage must appear [1]. Skid steering can be compact, light, require few parts, and exhibit agility from point turning to line driving using only the motions, components, and swept volume needed for straight driving. However, as the turn radius decreases from straight driving to a point turn, greater power and torque are required as a greater sideslip angle is encountered. For all turns skid steering requires greater power and torque than for explicit turning because sideslip angles are greater in all cases. The lateral forces of skid steering are greater [2][3][4]. Fig. 1 shows the skid steer and explicit steer.
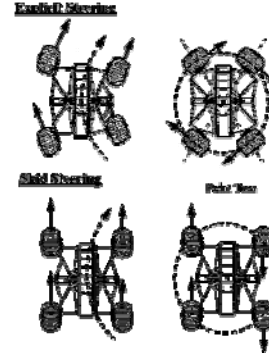
Fig. 1. Skid steer and explicit steer

Skid steering is accomplished by creating a differential velocity between the inner and outer wheels. There are three kinds of control strategies: with the inner wheels braked, by simultaneously speeding up the outer wheels and slowing down inner wheels, and by only speeding up the outer wheels [5]. It is found that the second method minimizes transients.

The increasing prospect of electric drive vehicles and the development of individual wheel traction motors, opens up the possibility of designing higher performance skid steer systems [5]. The use of separate traction motors at each wheel implies that torque to each drive wheel can be controlled independently. This kind of wheels are known as motorized wheels, which permit packaging flexibility by eliminating the central drive motor and the associated transmission and driveline components, including the transmission, the differential, the universal joints and the drive shaft [6]. So it provides a system that is regenerative by nature, by using motor braking, the power absorbed at one wheel is available for application at an opposing wheel.

By controlling the traction of each wheel individually, the vehicle yaw moment can be controlled directly [7]-[12]. However, perfect control of those independent motors will be a critical issue in this configuration.

In [6], a stability system in all-wheel-drive Electric Vehicle is introduced. The system comprises a fuzzy logic system that independently controls wheel torques to prevent vehicle spin. It also points out that yaw rate control of a vehicle by utilizing skid steering method is usually addressed as Direct Yaw-moment Control (DYC). It has been proved that DYC is more effective in enhancing vehicle stability than four wheel steering. Actually, the yaw moment resulting from difference in longitudinal tire force of left and right wheels is insignificantly influenced by lateral acceleration. On the contrary, the yaw moment generated by four-wheel steering decreases as the lateral acceleration increases.

The steering performance of a 4WD skid steer vehicle is presented in [5], the author states that the actual turn radius will be larger than the desired value because of the wheel slip.

In this paper, we develop a 4WD skid steering electric vehicle, which is driven by four separate induction motors in each wheel, Fig. 2 shows the configuration of the motorized wheels on one side of the vehicle. The unite semi-empirical tire model is developed here which is different from most papers in tire modeling where linear model is prevalent. To distribute the torque of each wheel well enough, the slip ratio is fed back to adjust the given speed of the driven motors, then the torque is distributed again in order to satisfy the driver command. The objective is to analyze the behavior of skid steering applied to 4×4 electric vehicles when the inner and the outer wheel are given different speeds, the main characteristics are based on maneuverability, stability and the accuracy.
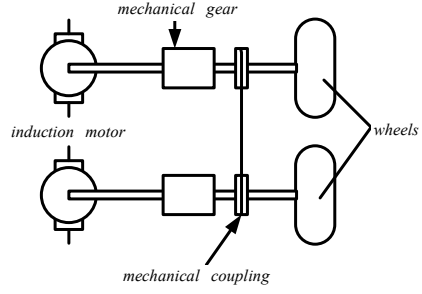

Fig. 2. Configuration of motorized wheel

II. SKID STEERING SYSTEM

The entire system consists of several models, including tire model, vehicle model, induction motor drive model and the slip limitation feedback controller.
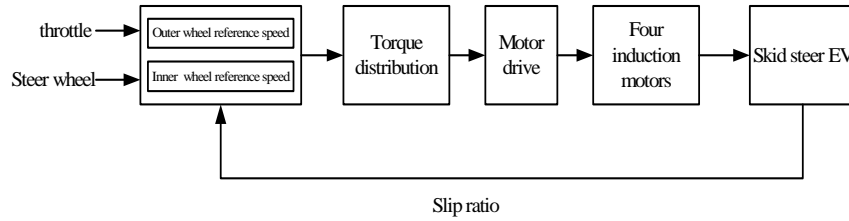
A. Entire System

Fig. 3. Entire system

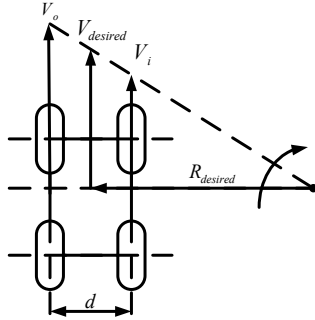Skid steering electric vehicle model is shown in Fig. 4.

Fig. 4. Skid steering electric vehicle model

The radius of the turn can be calculated from similar triangles

$$R_{desired} = \frac{V_o + V_i}{V_o - V_i} \cdot \frac{d}{2} \qquad (1)$$

$$V_{desired} = \frac{V_o + V_i}{2} \qquad (2)$$

Where $R_{desired}$ and $V_{desired}$ are the desired speed and the turn radius, V_o and V_i denote the desired outer wheel speed and the inner wheel speed respectively, d represents the distance of the left and the right wheel.

The input of the simulation system is the desired speed and the turn radius, then the inner and outer speed can be calculated from (1) and (2).

B. Tire Model

Regardless of the inability of the linear model to provide the wheel tractive force, which is the most important factor is that the linear model could not properly describe the overall vehicle dynamic behavior in some driving conditions. It is well known that the most accurate tire model is the magic formula model, developed by Bakker et al. But it is also the one requiring the longest computation time for the determination for the coefficients. The tire model used in this simulation study is relatively more complex than in a simple linear model, which is called unite semi-empirical tire model. From this model, longitudinal and lateral tire force can be calculated by slip ratio directly.

List of symbols:

μ —tire-road total friction coefficient

V_x —longitudinal tire speed

V_y —lateral tire speed

ω —wheel angular speed

F_z —normal force

R —tire radius

μ_0 —tire-road static friction coefficient

V_0 —speed constant

k_x —tire initial infinitude relative longitudinal stiffness

k_y —tire initial infinitude relative lateral stiffness

E_y —tire force characteristic parameter

F_f — roll friction

F_w — wind friction

F_x — longitudinal tire force

F_y — lateral tire force

m — mass of vehicle

I_z — moments of inertia about Z axis

lf — distance from front axle to CG

lr — distance from rear axle to CG

d — distance between the left and the right wheel

θ — yaw angle

M_f — roll resistance moment

J_w — moment of inertia

g — acceleration of gravity

h — height of CG

C_0 —wind block coefficient

A — wind area

γ — yaw rate

f — roll resistance coefficient

u — longitudinal speed of CG in fixed reference frame

v — lateral speed of CG in fixed reference frame

T_d —electromagnetic torque of induction motor

n_p —number of poles

The tire-road relative slip velocity V_s and friction coefficient μ can be calculated by longitudinal speed V_x and lateral vehicle speed V_y and the wheel angular speed ω which are illustrated in Fig. 5.
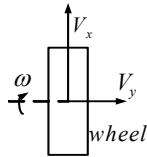

Fig. 5. Wheel speed

$$V_s = \sqrt{(V_x - \omega \cdot R)^2 + V_y^2} \qquad (3)$$

$$\mu = \mu_0 \cdot e^{-\frac{(V_x - \omega R)^2 + V_y^2}{V_0}} \qquad (4)$$

longitudinal slip

$$s_x = \frac{V_x - \omega R}{\omega R} \qquad (5)$$

lateral slip

$$s_y = \frac{V_y}{\omega R} \qquad (6)$$

infinitude relative longitudinal slip

$$\phi_x = \frac{k_x \cdot s_x}{\mu} \qquad (7)$$

infinitude relative lateral slip

$$\phi_y = \frac{k_y \cdot s_y}{\mu} \qquad (8)$$

infinitude total slip

$$\phi = \sqrt{\phi_x^2 + \phi_y^2} \qquad (9)$$

With (3)-(9), we get the longitudinal tire force and the lateral tire force (10), (11).

$$F_x = -\frac{\phi_x}{\phi} \cdot F_z \cdot \mu \cdot [1 - e^{-\phi - E_y \cdot \phi^2 - (E_y^2 + \frac{1}{12}) \cdot \phi^3}] \qquad (10)$$

$$F_y = -\frac{\phi_y}{\phi} \cdot F_z \cdot \mu \cdot [1 - e^{-\phi - E_y \cdot \phi^2 - (E_y^2 + \frac{1}{12}) \cdot \phi^3}] \qquad (11)$$

C. Vehicle Model

The coordinate system of the car shown in Fig. 6 is based at the bottom of the wheel where the X coordinate is in the direction of wheel travel. The Y coordinate is parallel to the axis of the wheel's rotation and the Z coordinate is perpendicular to the ground.
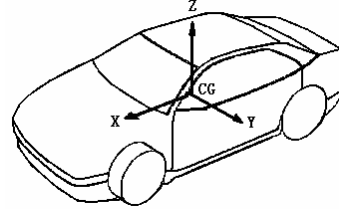

Fig. 6. Car coordinate system

We develop a vehicle dynamic model by neglecting some effects introduced by suspension and tire deformation.

The following assumptions are made:

1) Vehicle is moving on the horizontal plane
2) Vehicle speed is very low
3) Vehicle has no vertical motion
4) Vehicle has no pitch motion about Y axis or roll motion about X axis

Referring to Fig. 7, $O(X, Y)$ defines a fixed reference frame and $CG(x, y)$ is a moving frame attached to the vehicle body with origin at the center of mass CG. The center of mass is located at distances lf and lr from front and rear wheels respectively. The distance of left and right wheel is d.

The weight transfers are taken into consideration in the vehicle model. The lateral tire forces are thought of as causing resistance to turning, which is overcome by the differential longitudinal (or tractive) forces between the two sides of the vehicle. The lateral and longitudinal tire force induced yaw moments are balanced to provide the indicated yaw acceleration.
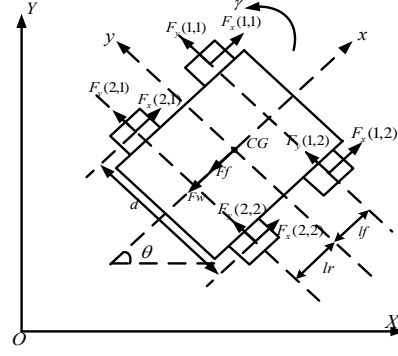
Fig. 7. Motion frame of skid steer EV

The 3-DOF motion equations in the moving frame can be written in (12)-(14), where the subscript (1,1), (1,2), (2,1) and (2,2) indicate the front left (FL) wheel, the front right (FR) wheel, the rear left (RL) wheel and the rear right (RR) wheel separately.

Longitudinal:

$$m(\dot{u} - \gamma \cdot v) = F_x(1,1) + F_x(1,2) + F_x(2,1) + F_x(2,2) - F_f - F_w$$

(12)

Lateral:

$$m(\dot{v} + \gamma \cdot u) = F_y(1,1) + F_y(1,2) + F_y(2,1) + F_y(2,2)$$

(13)

Yaw:

$$I_z \cdot \dot{\gamma} = [F_y(1,1) + F_y(1,2)] \cdot lf - [F_y(2,1) + F_y(2,2)] \cdot lr$$

$$- \frac{d}{2}[F_x(1,1) - F_x(1,2) + F_x(2,1) - F_x(2,2)]$$

(14)

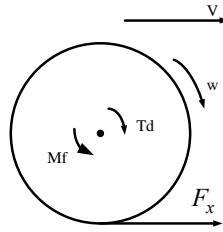We can also get the torque equilibrium equations (15) of the four wheels from moments on a wheel in Fig. 8.

Fig. 8. Moments on a wheel

$$J_w \cdot \dot{\omega}(1,1) = T_d(1,1) - F_x(1,1) \cdot R - M_f(1,1)$$

$$J_w \cdot \dot{\omega}(1,2) = T_d(1,2) - F_x(1,2) \cdot R - M_f(1,2)$$

$$J_w \cdot \dot{\omega}(2,1) = T_d(2,1) - F_x(2,1) \cdot R - M_f(2,1)$$

$$J_w \cdot \dot{\omega}(2,2) = T_d(2,2) - F_x(2,2) \cdot R - M_f(2,2)$$

(15)

The longitudinal speed and lateral speed of each wheel are given by (16).

D. Induction Motor Drive

Vector control of induction motors has been widely used in high performance drive system. Field oriented

$$V_x(1,1) = u - \gamma \cdot \frac{d}{2} \qquad V_y(1,1) = v + \gamma \cdot lf$$

$$V_x(1,2) = u + \gamma \cdot \frac{d}{2} \qquad V_y(1,2) = v + \gamma \cdot lf$$

$$V_x(2,1) = u - \gamma \cdot \frac{d}{2} \qquad V_y(2,1) = v - \gamma \cdot lr$$

$$V_x(2,2) = u + \gamma \cdot \frac{d}{2} \qquad V_y(2,2) = v - \gamma \cdot lr$$

(16)

The equations (17)-(23) can be derived from the vehicle locomotion

$$M_f(i.j) = F_z(i,j) \cdot f \cdot (1 + \frac{u^2}{1500}) \cdot R$$

(17)

$$F_z(1,1) = \frac{m}{lf+lr}[\frac{1}{2}g \cdot lr - \frac{1}{2}(\dot{u} - \gamma \cdot v) \cdot h + \frac{(\dot{v} + \gamma \cdot u) \cdot h \cdot lr}{d}]$$

$$F_z(1,2) = \frac{m}{lf+lr}[\frac{1}{2}g \cdot lr - \frac{1}{2}(\dot{u} - \gamma \cdot v) \cdot h - \frac{(\dot{v} + \gamma \cdot u) \cdot h \cdot lr}{d}]$$

(18)

$$F_z(2,1) = \frac{m}{lf+lr}[\frac{1}{2}g \cdot lf + \frac{1}{2}(\dot{u} - \gamma \cdot v) \cdot h + \frac{(\dot{v} + \gamma \cdot u) \cdot h \cdot lr}{d}]$$

$$F_z(2,2) = \frac{m}{lf+lr}[\frac{1}{2}g \cdot lf + \frac{1}{2}(\dot{u} - \gamma \cdot v) \cdot h - \frac{(\dot{v} + \gamma \cdot u) \cdot h \cdot lr}{d}]$$

)

$$F_w = \frac{1}{21.15} \cdot C_0 \cdot A \cdot u^2$$

(19)

$$F_f = m \cdot g \cdot (1 + \frac{u^2}{1500})$$

(20)

The heading angle

$$\theta = \int \gamma \cdot dt$$

(21)

The longitudinal displacement in fixed reference frame

$$X = \int (u \cdot \cos\theta - v \cdot \sin\theta)dt$$

(22)

The lateral displacement in fixed reference frame

$$Y = \int (-u \cdot \sin\theta - v \cdot \cos\theta)dt$$

(23)

induction motor drive systems offer high performance as well as independent control on torque and flux. The rotor flux field oriented vector control has been used as the induction motor drive method.

E. Slip Limitation Feedback Controller

Desired turn radius will only be achieved if no slippage occurs between the wheel and ground [5], to satisfy the requirement of the turn radius, the longitudinal slip must be controlled, so a method of slip limitation feedback is used in the simulation.

The desired turn radius is given in (1).

The desired yaw rate

$$\gamma_{desired} = \frac{V_o - V_i}{d} \qquad (24)$$

Where V_o and V_i denote the desired outer wheel speed and the inner wheel speed respectively, d represents the distance of the left and the right wheel.

Therefore

$$V_o = \omega_o \cdot R \qquad (25)$$
$$V_i = \omega_i \cdot R \qquad (26)$$

Where ω_o and ω_i represent outer and inner wheel angular speed.

As is mentioned before, the longitudinal slip of the wheel is

$$s_x = \frac{V_x - \omega R}{\omega R} \qquad (27)$$

That is to say,

$$V_x = (s_x + 1) \cdot \omega R \qquad (28)$$

The actual turn radius will be

$$R_{actual} = \frac{V_o(1 + s_o) + V_i(1 + s_i)}{V_o(1 + s_o) - V_i(1 + s_i)} \cdot \frac{d}{2} \qquad (29)$$

The actual yaw rate

$$\gamma_{actual} = \frac{V_o(1 + s_o) - V_i(1 + s_i)}{d} \qquad (30)$$

When the vehicle turns, the outer wheel accelerates and the inner wheel decelerates, that is to say, for the outer wheel, the wheel rotate speed is greater than the wheel line speed, and for the inner wheel, the case is just reverse. So the longitudinal slip of the outer wheel s_o is less than zero, and the inner wheel slip s_i is greater than

zero, from the equation of the actual turn radius, we can conclude that actual difference between the outer and inner speed will be less than the desired value, so the actual turn radius and yaw rate will be smaller than the desired values.

To satisfy the requirements of the turn radius and the yaw rate, the difference between the outer and inner speed must be controlled.

To increase the reference speed of the outer wheel and the inner wheel, the method of slip limitation feedback is used here. Firstly, the longitudinal slips of the four wheels are calculated and fed back to the reference speed controller, in the controller, the slips are limited to a range, then the reference speed are revised to a new value, and the output torque of the induction motor will be revised until the turn radius and the yaw rate reach to the desired values.

The reference speed are revised to

$$V_{oreference} = \frac{V_o}{1 + s_o} \qquad (31)$$

$$V_{ireference} = \frac{V_i}{1 + s_i} \qquad (32)$$

Replacing V_o and V_i in (1) and (24) by $V_{oreference}$ and $V_{ireference}$ respectively in the equations of actual turn radius and the yaw rate, then the actual turn radius and the yaw rate will be equal to the desired value.

III. SIMULATION RESULTS

Fig. 10 shows locus of the EV for different turn radius with tire-road friction coefficient is 0.8, and Fig. 11 to 14 illuminate the torque requirement for different turn radius for each wheel. We can see that the actual turn radius is well accordant with desired command from the driver, and as the turn radius becomes smaller the more torque is needed for each wheel at some constant speed.
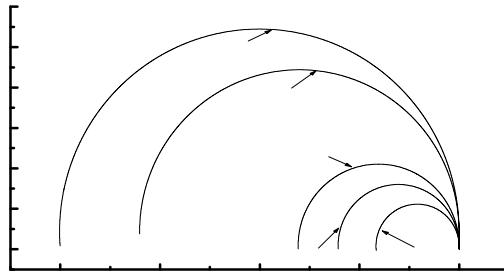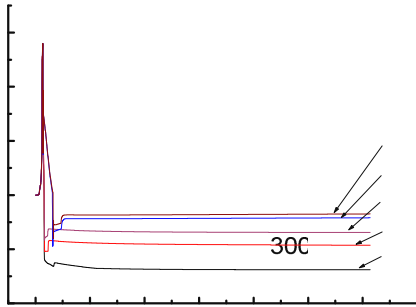
Fig. 10. Locus of the EV for different turn radius

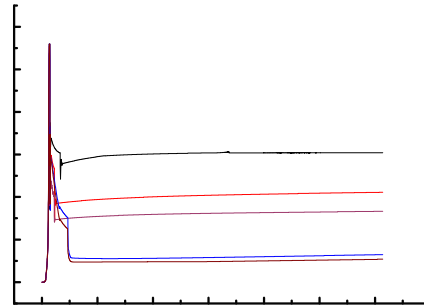Fig. 11. Torque requirement of the FL wheel for different turn radius

Fig. 12. Torque requirement of the FR wheel for different turn radius
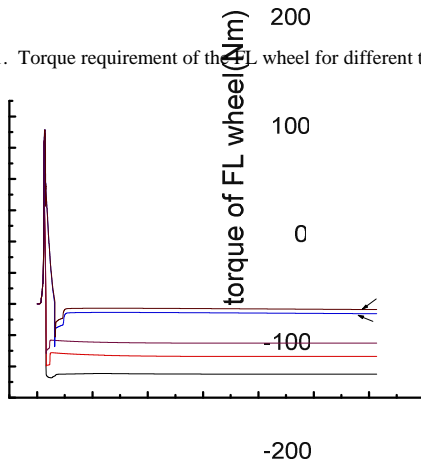
turn radius=10m

turn radius=8m

turn radius=4m

turn radius=3m

turn radius=2m

Fig. 13. Torque requirement of the RL wheel for different turn radius
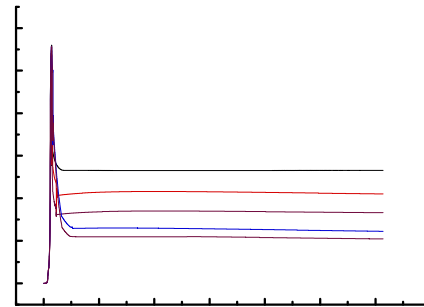
Fig. 14. Torque requirement of the RR wheel for different turn radius

IV. CONCLUSIONS

The paper describes a model for predicting the steering performance of a 4WD skid steer wheeled vehicle. The unite half-experience tire model is used here, which is more elaborate and the longitudinal and lateral tire force can be calculated by slip ratio directly. Induction motor is chosen as the driven motor, and the control method is rotor flux field oriented vector control. Slip limitation feedback controller is used to satisfy the requirement of the turn radius and the yaw rate. The simulation results show that the steering accuracy and maneuverability can be achieved, and the traction control system can adjust the motor torque to satisfy different road conditions.

V. REFERENCES

[1] D. Pazderski, K. Kozlowski, M. Lawniczak, "Practical stabilization of 4WD skid steering mobile robot," Proc. of the Fourth International Workshop on Robot Motion and Control, Puszczykowo, pp. 175-180, 2004.

[2] Benjamin Shamah, "Experimental Comparison of Skid Steering Vs. Explicit Steering for a Wheeled Mobile Robot," master's thesis, tech. report CMU-RI-TR-99-06, Robotics Institute, Carnegie Mellon University, March, 1999.

[3] E. Faruk Kececi, Gang Tao, "Adaptive vehicle skid control," Mechatronics 16 (2006) 291–301.

[4] Krzysztof, Kozowski, Dariusz, Pazderski, "Modeling and Control of 4wheel skid-steering mobile robot, " Int. J. Appl. Math. Comput. Sci., 2004, Vol. 14, No. 4, 477–496.

[5] Villiam R. Meldrum, Francis B.Hoogterp, Alexander R.Kovnat, "Modeling and Simulation of a Differential Torque Steered Wheeled Vehicle, " Technical Report 13777 July 1999.

[6] Farzad Tahami, Reza Kazemi and Shahrokh Farhangh, "A novel driver-assist stability system for all-wheel-drive Electric Vehicles," *IEEE TRANSACTIONS ON VEHICULAR TECHNOLOGY*, VOL. 52, NO. 3, MAY 2003.

[7] R.E. Colyer, J.T. Economou, "Soft modeling and fuzzy logic control of wheeled skid-steer electric vehicles with steering prioritization, " International Journal of Approximate Reasoning 22 (1999) 31-52.

[8] Guilin Tao, Zhiyum Ma, Libing Zhou, Langru Li., "A novel driving and control system for direct-wheel-driven electric vehicle, " *Magnetics, IEEE Transactions on.* Jan. 2005 Volume: 41, Issue: 1, Part 2 pp.497 – 500.

[9] U-Sok Chong, Eok Namgoong, Seung Ki Sul, "Torque steering control of 4-wheel drive electric vehicle" Power Electronics in Transportation, 1996. IEEE. pp. 159 – 164.

[10] Sakai S, Sado H, Hori Y, "Motion control in an electric vehicle with four independently driven in-wheel motors," *Mechatronics, IEEE/ASME Transactions on* March 1999 Volume: 4, Issue: 1, pp. 9 – 16.

[11] Pusca, R. Ait-Amirat, Y. Berthon, A. Kauffmann, J.M. CREEBEL, "Modeling and simulation of a traction control algorithm for an electric vehicle with four separate wheel drives," Vehicular Technology Conference, 2002. Proceedings. VTC 2002-Fall. 2002 IEEE 56th, pp. 1671 - 1675 vol.3.

[12] Jalili-Kharaajoo, M. Besharati, F., "Sliding mode traction control of an electric vehicle with four separate wheel drives," Emerging Technologies and Factory Automation, 2003. Proceedings. ETFA '03. IEEE Conference Sept. 2003 Volume: 2 , pp. 291 - 296.

torque of FL wheel(Nm)

torque of RL wheel(Nm)

Time(s)

turn radius=10m

turn radius=8m

turn radius=4m

turn radius=3m

turn radius=2m

Time(s)